Formation and Evolution process of Giant Molecular Clouds in the Large Magellanic Cloud




◎Yasuo Fukui, Miyuki Murai, Hinako Iritani, Akiko Kawamura, Tony Wong,
Yoji Mizuno, Erik Muller, Norikazu Mizuno, Toshikazu Ohnishi,
L. Staveley-Smith, S.Kim

1. Introduction

The Magellanic system including the Large and Small Magellanic Cloud (LMC, SMC) and the Magellanic Bridge is an ideal laboratory to study star formation and cloud evolution. In particular, the LMC offers the best site because of its proximity and its nearly face-on view. Among the various objects in the LMC, molecular clouds which are probed most easily using CO mm emission, provide a key to understand star formation and galaxy evolution. This is because molecular clouds are able to highlight region of star formation due to their relatively compact distribution both in space and in velocity. The situation is contrasted with atomic hydrogen gas which has a generally lower density and more loosely coupled to star formation.The key issue is the relationship of the molecular clouds with the HI. GMCs are the major sites of the star formation and the GMC formation must be a crucial step in the evolution of a galaxy. In order to better understand the relationship of the molecular and neutral hydrogen phase, we compared CO and HI emission in the LMC in 3-dimensional space revealing the physical connection between GMCs and associated HI gas at a ~40 pc scale.

2. Three Types of GMC

A comparison of physical parameters indicates that size and mass tend to increase from Type I to Type III, and Type III. GMC has the largest size and mass among the three. The stage after Type III is perhaps a very violent dissipation of GMCs due to UV photons and stellar winds from formed clusters.

Figure 1.

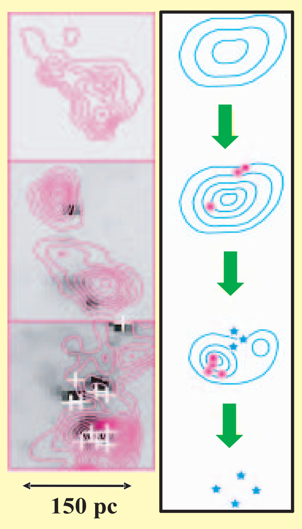

Type I (~6Myr) no apparent sign of star formation

Type II (~13Myr) associated with small HII regions only but without stellar clusters

Type III (~6Myr) most actively forming stars as shown by huge HII regions and young stellar clusters

Fukui et al. (2001, 2007)

3. Comparison between HI and CO

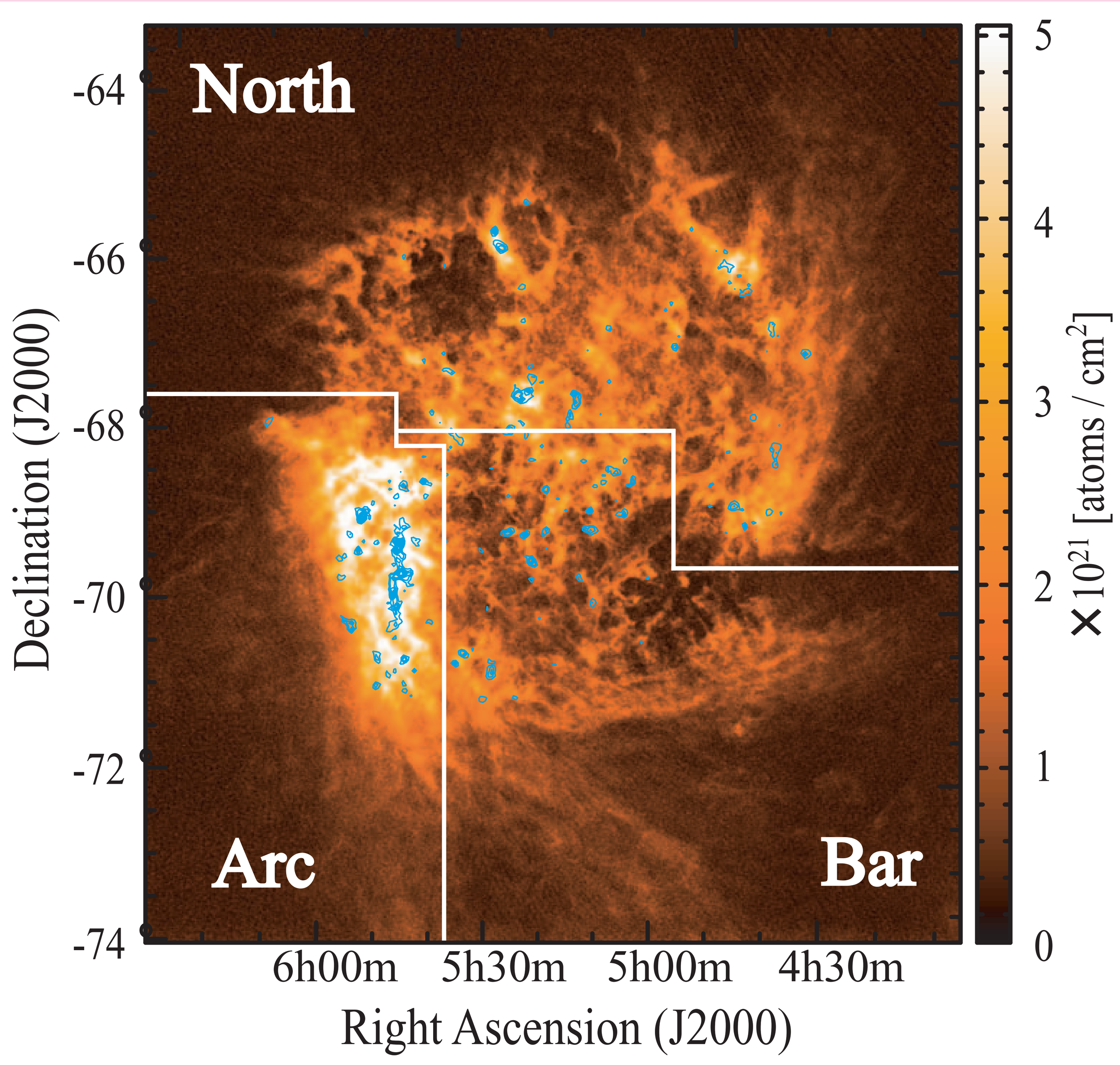

Observational Data;

CO (J=1-0): NANTEN

HI : ATCA and Parkes

- HPBW = 2'.6 (40 pc)
- Velocity Resolution = 1.65 km/s

Figure 2.
HI image (Kim et al. 2003) with the CO contours (Fukui et al. 2007). The contours are from 1.2 K km/s with 3.6 K km/s intervals.
We divided the whole region into three; Bar, Arc, and North.

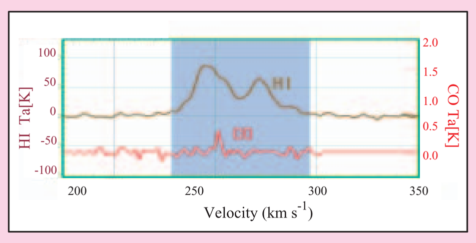

HI and CO profiles at
(5h 35m 42s), (-69 ° 11' 12") (J2000)

3.1. Distribution of HI Intensity

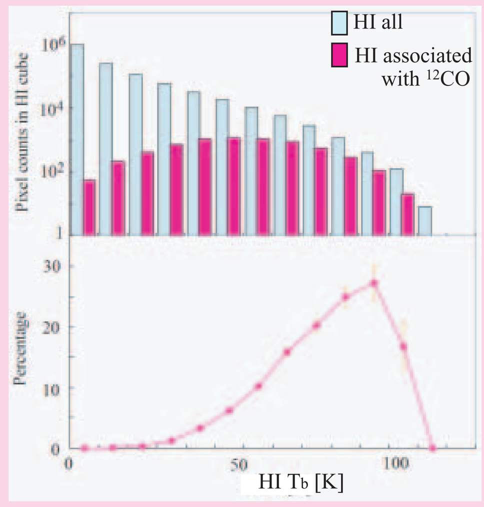

Figure 3.
Upper Panel
Distribution of HI integrated intensity in 3-D where the significant CO emissions are detected.
Lower Panel
The ratio of the HI pixels with and without CO mission.

Figure 3 shows that the CO fraction increases steadily with the HI intensity, suggesting the HI provides a necessary condition to form GMCs. About one third of the pixels exhibit CO emission near T_b(HI) of ~ 90 K (2.6×10^{20} cm^{-2}) and it seems that there is no sharp threshold value for GMC formation with respect to the HI intensity.

3.2. Distribution of the HI T_b

Figure 4 shows that the HI intensity tends to increase from Type I to Type III. The average HI intensity over the whole LMC is 34±16 K, 47±17 K and 56±19 K for Type I, II and III, respectively. The HI intensity surrounding the GMCs becomes greater with the GMC evolution and star formation. In order to test the variation within the galaxy, we shall divide the galaxy into three regions.

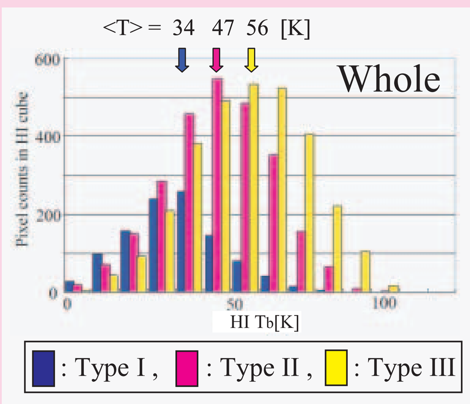

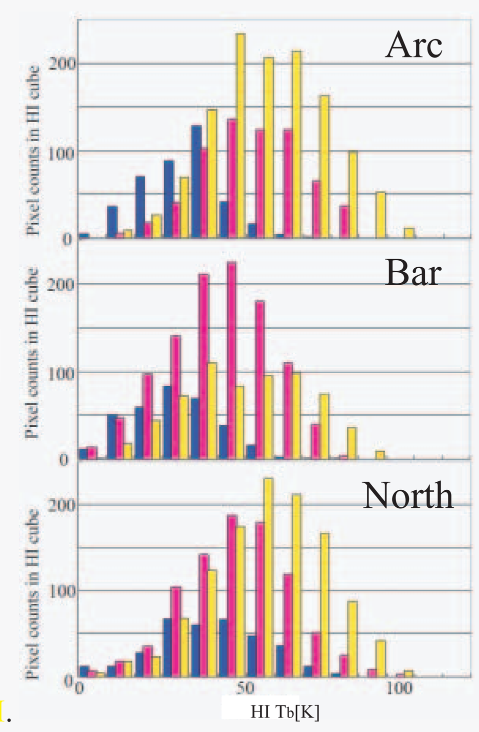

Figure 4.
Distribution of the HI antenna temperature(Ta) associated with the GMCs in the entire galaxy, the arc, the bar, and the north regions from the top. Each panel indicates the HI intensity distribution associated with the GMC Type I, Type II, and Type III.

3.3. Examples of the HI and CO distributions of the GMC

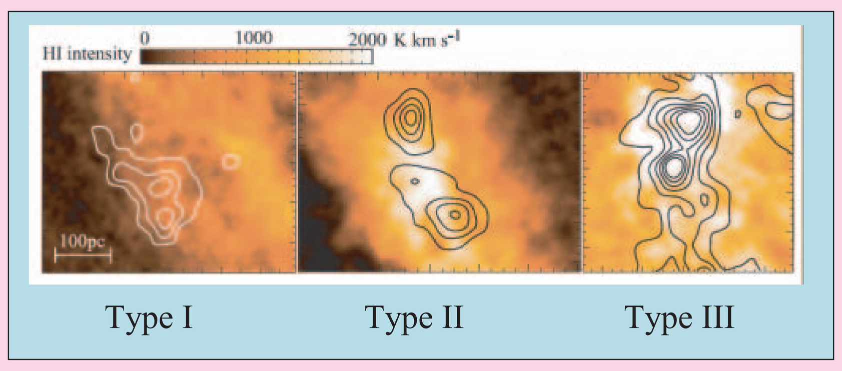

Figure 5.
Examples of the HI and CO distributions of the each GMC Types. Images are HI integrated intensity maps; velocity is integrated over the range where the significant CO emissions are detected. The contours are CO integrated intensities from 1.2 [K km/s] with 1.2 [K km/s] intervals (Fukui et al. 2007).

The CO distribution has detailed structures of ~ 40 pc or less and the HI seems to be associated with the GMC at a scale of 50-100 pc. The HI is not always isotropic with respect to a GMC but indicates close spatial correlations so that the HI is more or less enveloping a GMC. The HI that is associated with the CO typically has velocity width of ~10-14 km s^{-1}. Broader peaks are generally becomes much weaker.

3.4. Correlation between the HI and the CO intensities

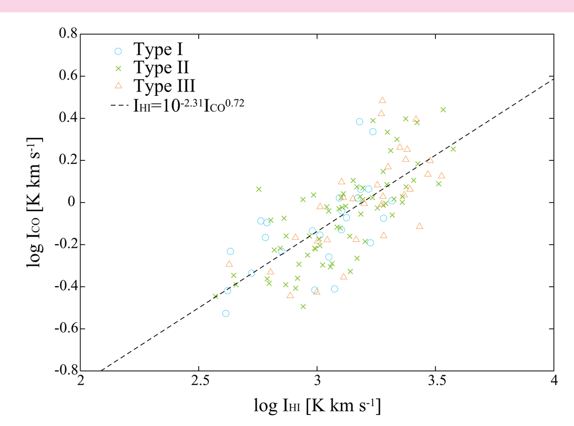

Figure 6.
This diagram indicates correlation between HI and CO intensities. Open circles, crosses and open triangles represent each the GMC Types. The dotted line shows the regression line of $I_{CO} = 10^{-2.31} I_{HI}^{0.72}$.

We had selected 124 GMCs in the LMC and estimated their L_{CO}. We then divided the L_{CO} by the apparent size of a GMC. This gives an average CO intensity. I_{HI} is summed over $V_{CO} \pm 0.5 \times \Delta V_{CO}$. The regression shown in Figure 6 is well fitted by a power law with a negative index of ~ 0.7, indicating a nearly linear correlation between CO and HI in a GMC.

3.5. Dressed GMCs; Growth of GMCs via HI Accretion

The HI intensity is generally a product of the spin temperature and the optical depth, and the correlation indicates temperature and/or density is dependent on Type. We infer that GMCs are "dressed" in HI and that the "HI dress" grows in time. The correlation between the HI and the CO is nearly linear (Figure 6). This alone does not provide a strong constraint on the formation of a GMC. Nonetheless, the apparent association of HI with GMCs suggests that the HI is enveloping each GMC and the HI density increases with the cloud evolution. We infer that this represents the enveloping HI gas is accreting onto GMCs and is converted into H_2 due to increased optical depth. This leads to increase the molecular mass of GMC, i.e., the observed mass increase from Type I to III. We fitted gaussian profile to the CO and the HI spectra, and compared center velocity. The timescale of the GMC evolution is ~10 Myrs and the increased molecular mass is in the order of 10^6 M_{solar}. Namely, a mass accretion rate of ~10^{-1} M_{solar} yr^{-1} is required. We estimated that this rate is consistent with that calculated for a spherical accretion of the HI gas having n(HI) ~10 cm^{-3} at an infall speed of ~7 km s^{-1}.

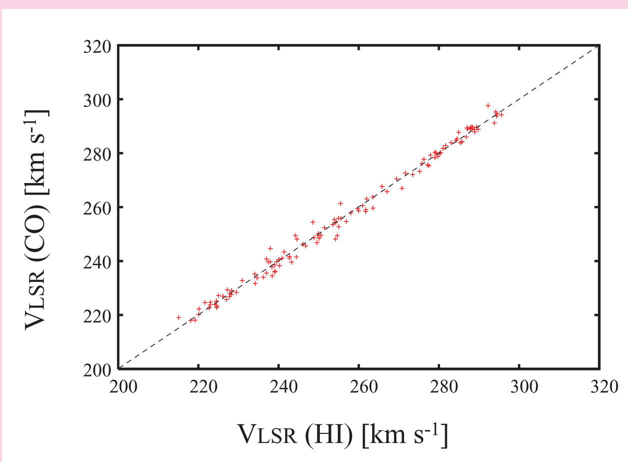

Figure 7
This figure shows correlation between V_{LSR}(CO) and V_{LSR}(HI) derived from fitted gaussian profile. In the dotted line, both V_{LSR} is an equal.

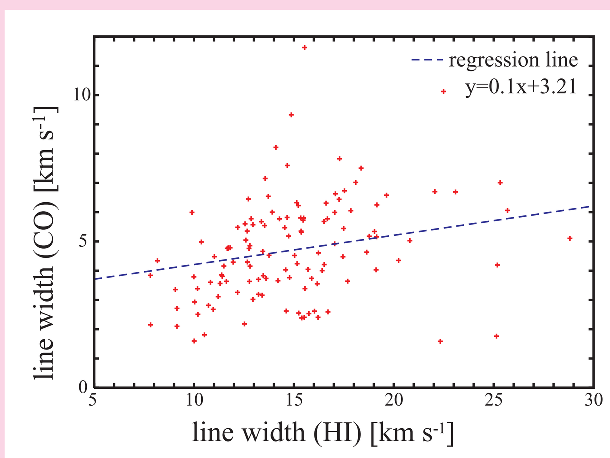

Figure 8
This figure shows correlation between CO and HI line width. These are derived from fitted gaussian profile.

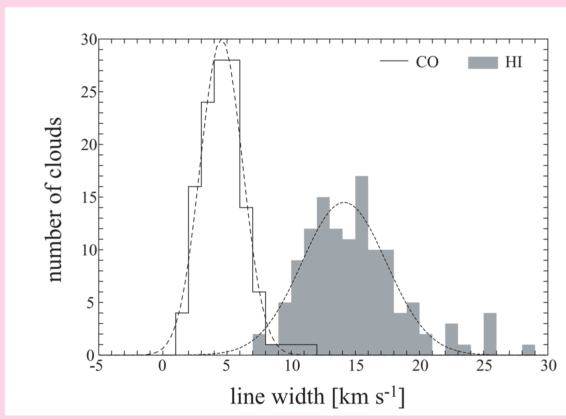

Figure 9
This figure is a number histogram of line width of CO and HI. The clouds in this histogram are selected clouds. The dotted lines are well fitted by Gaussian. The mean and the standard derivation of CO and HI are 4.6, 1.6, 14.1, 3.3 respectively.

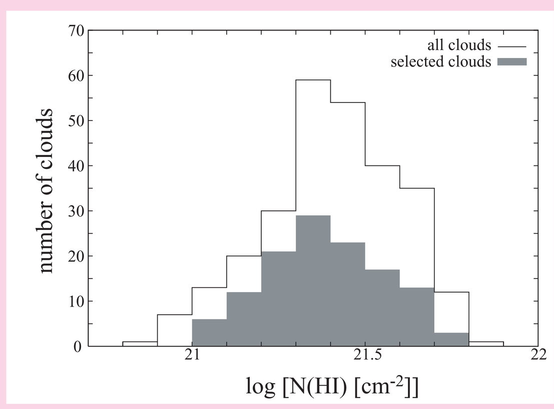

Figure 10
Distribution of HI column density
The outline box shows the entire clouds and hatched region shows the 124 selected clouds.

4. Summary

Three-dimensional comparison between CO and HI has revealed GMCs are associated with HI gas at a ~40pc scale; these are "HI dressed GMCs". There is a clear increase of the HI intensity around GMCs from GMC Type I to Type III. Growth of GMCs in mass via HI accretion has been suggested over a time scale of a few ~10 Myrs. This correlation has a form, [CO intensity]∝[HI intensity]$^{0.8}$, for selected 118 major GMCs. The timescale of the GMC evolution is ~10 Myrs and the increased molecular mass is in the order of 10^6 M_{solar}. Namely, a mass accretion rate of ~10^{-1} M_{solar} yr^{-1} is required. We estimated that this rate is consistent with a spherical infall at a rate of ~7 km s^{-1}.

References

Fukui, Y. et al. 1999, PASJ, 51, 745
Fukui, Y. 2001a, PASJ, 53, 959
Fukui, Y. 2001b, PASJ, 53, 985
Fukui, Y. et al. 2008, arXiv, 0804,1458
Kim, S. et al. 1999, AJ, 118, 2797
Kim, S. et al. 2003, APJS, 148, 473